ISSN: 2414-1895 DOI: 10.6919/ICJE.202503_11(3).0004

Dual-core Photonic Crystal Fiber in the Terahertz Band of Cancer Cell Biodetection Sensor

Jinpei Wang, She Li*, Han Ding, and Yingying Song

School of Science, Heilongjiang University of Science and Technology, Harbin 150040, China

*Corresponding author email: lishe1979@163.com

Abstract

Terahertz waves are used in non-destructive testing and biosensing due to their special transparency and safety, while photonic crystal fibers are used to fabricate various optical devices due to their unique optical transmission characteristics. This article studies a dual core terahertz photonic crystal fiber biological detection sensor, which introduces elliptical air holes between two fiber cores, and the cladding is composed of elliptical air holes of the same size arranged in a hexagonal pattern. Using finite element method for research, normal blood cells and cancerous blood cells are used as test objects to study and analyze the coupling length and coupling length ratio of optical fibers in the frequency range of 0.5THz-1.1THz. The results show that by optimizing the structural parameters of photonic crystal fibers, a shorter coupling length of 182.27 μm and a normalized output power change of 91.26% were obtained, which has important application potential in the fields of biosensing and medical detection.

Keywords

Photonic Crystal Fibers; Terahertz; Biosensor.

1. Introduction

In recent years, terahertz waves have attracted considerable attention from researchers due to their unique properties, such as low photon energy, high signal-to-noise ratio, and broad bandwidth [1]. Terahertz waves are located between microwaves and infrared in the electromagnetic spectrum, with frequencies ranging from 0.1 THz to 10 THz (wavelengths between 30 μm and 3 mm) [2]. The wavelength of terahertz waves is situated in the transition zone between photonics and electronics, lying between macroscopic and microscopic electronics. Their characteristics include low photon energy and strong penetration ability [3]. Photonic crystal fibers are a special type of optical waveguide, which, as a periodic structure, such as hollow photonic crystal fibers, allow terahertz waves to propagate through them while minimizing certain losses. As a result, photonic crystal fibers provide a new method for controlling and guiding terahertz waves.

Photonic crystal fiber (PCF), also known as microstructured optical fiber, was first proposed by Russell et al. in 1992 [4]. The fiber's cladding consists of a regular arrangement of air holes, while the core is made up of silica and air-hole defects, which effectively confine the light within the core for propagation. Based on the guiding principles, PCF can be categorized into two types: the total internal reflection type and the photonic bandgap type.

PCF exhibits characteristics such as high birefringence, ultra-flattened dispersion, single-mode transmission without cutoff, and nonlinear effects, making it suitable for the fabrication of various optical devices [5]. Currently, the use of gases, liquids, and other materials filled into the core or air holes of photonic crystal fibers has been widely applied in various fields, including biosensing [6] and optical communications [7], demonstrating the broad application prospects of photonic crystal

ISSN: 2414-1895 DOI: 10.6919/ICJE.202503_11(3).0004

fibers. Cancer is a disease that cannot be completely cured with medication, making early diagnosis particularly important. Researchers have been striving to develop rapid cancer cell detectors [4]. Cancer cells and normal cells exhibit different refractive indices (RI) and display distinct propagation characteristics when illuminated with light from similar sources. These differences can be detected by studying the received signals, allowing for the identification of these distinct properties [8].

Khalid Mohd Ibrahimi and colleagues designed a biosensor based on a graphene, gold (Au), and titanium dioxide (TiO_2) layer hybrid, using a hexagonal lattice structure optical fiber with circular air holes drilled into the fiber to further enhance the sensor's performance. The research results indicate that after optimizing the fiber structure, the sensor demonstrated the highest sensitivity to MCF7 breast cancer cells under wavelength interference methodology [9].Md. Ranju Sardar and colleagues proposed a novel sensor based on photonic crystal fiber (PCF). The sensor design involves the precise chemical vapor deposition (CVD) technique to deposit gold (Au), a plasmonic material, onto the parallel and opposite outer edges of the PCF lattice. The PCF-SPR sensor is placed in a solution containing the cancer cells to be detected. An external detection system continuously monitors the sensor, allowing for the precise measurement of the refractive index of the detected cancer cells [10].Ram Pravesh, Dharmendra Kumar, and colleagues proposed a dual-D-shaped dual-core biosensor based on photonic crystal fiber (PCF) for cell detection. In this sensor, small circular holes in the middle create two independent waveguides, and it consists of two solid cores. The small circular hole in the center serves as the sensing channel, where blood components are placed. Due to the differing refractive indices of the blood samples, the peak wavelength of the transmission curve shifts, enabling the detection of blood components [11].However, these structures are complex, difficult to fabricate, and require high precision for sensing. To achieve more accurate and convenient cell type detection and better transmission performance, based on the aforementioned research, this paper investigates a PCF biosensor with a rectangular strip added to the fiber core and an elliptical air hole in the cladding. Using the finite element method, the refractive indices of normal blood cells and leukemia cells are used as the basis for measurement. The impact of structural parameters in the 0.5-1.1 THz frequency range on the coupling length and coupling ratio is studied, resulting in a PCF biosensor with good sensing performance.

2. Optical Fiber Structure and Theoretical Basis

2.1 Optical Fiber Structure

This paper studies a structurally simple dual-core photonic crystal fiber. The schematic diagram of the fiber structure cross-section and an enlarged view of the fiber core are shown in Fig. 1. The cladding consists of elliptical air holes of the same size, arranged in a triangular lattice pattern. The long axis of the elliptical air holes is a_1, and the short axis is b_1, with $\eta=b_1/a_1$. A rectangular strip is added in the fiber core, and the long axis of the elliptical air holes between the two cores is a_2, and the short axis is b_2. The base material used is ring-opening copolymer Topas (n = 1.5258), and the refractive index of the substance to be measured is calculated by adding it to the fiber core.

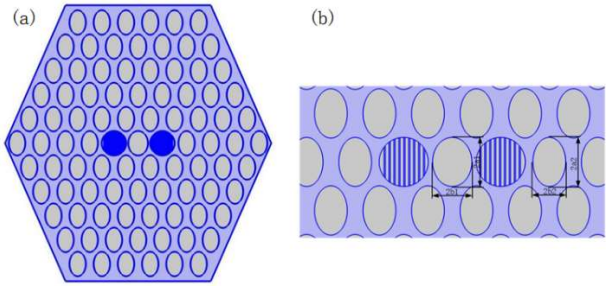

Fig. 1 Schematic Diagram of the Optical Fiber Structure and Enlarged View of the Fiber Core
(a)Schematic Diagram of Photonic Crystal Fiber Structure
(b)Enlarged Schematic Diagram of the Fiber Core

ISSN: 2414-1895 DOI: 10.6919/ICJE.202503_11(3).0004

2.2 Theoretical Basis

The Finite Element Method (FEM) can accurately calculate the mode field distribution and transmission characteristics of optical fibers with arbitrary cross-sectional shapes and refractive index distributions, making it highly suitable for the analysis of photonic crystal fibers [13]. Starting from Maxwell's equations, electromagnetic separation leads to the wave equation that the electric field satisfies:

$$\nabla \times \left(\mu_{\mathrm{r}}^{-1} \nabla \times \vec{E}\right) - \mathrm{k}_0^2 \varepsilon_{\mathrm{r}} \vec{E} = 0 \tag{1}$$

In equation (1), ε_r and μ_{r} represent the relative permittivity and relative permeability, respectively, and k_0 represents the wave number in vacuum. The light propagating along the Z-axis in the optical fiber takes the following form:

$$\vec{E}(x, y, z) = \vec{E}(x, y) \exp(-i\beta z) \tag{2}$$

In equation (2), β is the propagation constant. By solving equations (1) and (2) simultaneously and applying boundary conditions, the propagation constant β and the optical field distribution within the fiber cross-section can be theoretically determined. This allows for the calculation of the effective mode refractive index at the corresponding wavelength.

$$\mathrm{n}_{eff} = \frac{\beta}{k_0} \tag{3}$$

The coupling length (CL) refers to the shortest distance at which maximum power transfer occurs between the two cores [14]. The coupling lengths of the x-polarized mode and y-polarized mode, CLx and CLy, can be expressed as:

$$CL_{x,y} = \frac{\pi}{\beta_{even}^{x,y} - \beta_{odd}^{x,y}} = \frac{\lambda}{2\left(n_{even}^{x,y} - n_{odd}^{x,y}\right)} \tag{4}$$

In the equation, λ is the operating wavelength, and even, $\beta_{even}^{x,y}$ and $\beta_{odd}^{x,y}$, x are the propagation constants of the even and odd modes in the x-direction, while even, and y are the propagation constants of the even and odd modes in the y-direction. $n_{even}^{x,y}$, x ,and odd, are the refractive indices of the even and odd modes in the x-direction, and even, $n_{odd}^{x,y}$,y and odd, are the refractive indices of the even and odd modes in the y-direction.

To fully separate the x and y polarization modes, the physical length of the device must satisfy a sufficient condition, $L = \mathrm{n}CLR\mathrm{n} = \mathrm{m}CLR\mathrm{u}$, where m and n are positive integers with opposite parity [15]. The definition of the Coupling Length Ratio (CLR) is given by [16]:

$$CLR = \frac{\mathrm{m}}{\mathrm{n}} \tag{5}$$

ISSN: 2414-1895 DOI: 10.6919/ICJE.202503_11(3).0004

3. Simulation and Discussion

The mode field distributions of the four fundamental modes, when the core is filled with normal blood cells having a refractive index of n=1.376 and a frequency of 1.1 THz, are shown in Figure 2(a), (b), (c), and (d).

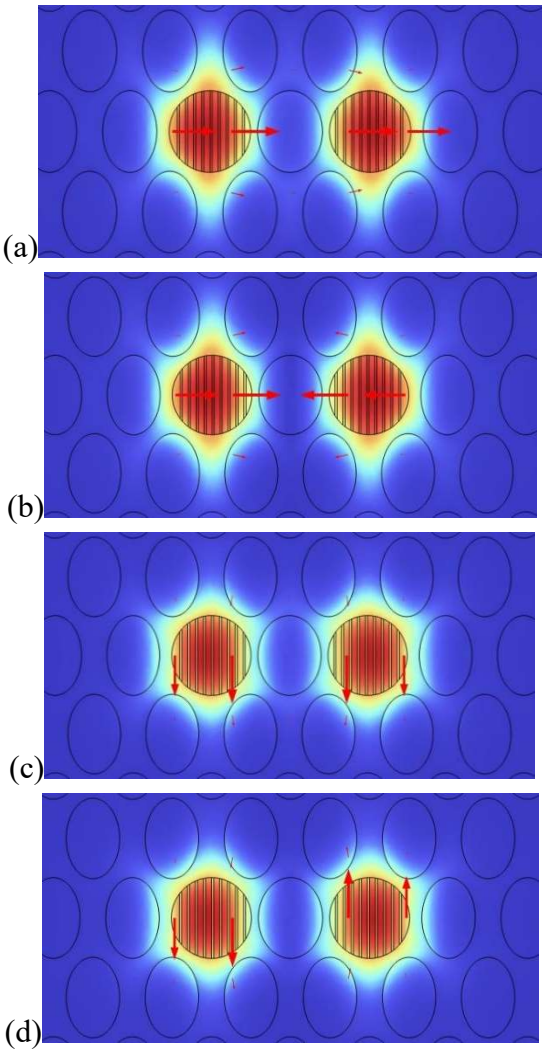

Fig. 2 Mode field distributions. (a) x-even mode; (b) x-odd mode; (c) y-even mode; (d) y-odd mode.

Fig. 2 shows the mode field distributions of the four fundamental modes. It can be observed that the energy is well confined within the two cores. This is due to the fact that the refractive index of the Topas material, which serves as the background, is 1.5258, while the refractive index of the normal blood cells filled in the cores is 1.376, and the refractive index of the cladding air holes is 1. When light propagates from the core to the cladding, total internal reflection effectively confines the light within the core. This demonstrates that the structure has a strong light confinement effect.

Fig. 3 shows that within the frequency range of 0.5-1.1 THz, the effective refractive index of the modes increases with the frequency. The effective refractive index of the x-polarized even mode reaches a maximum of 1.3638, followed by the y-polarized even mode at 1.3551, while the effective refractive index of the y-polarized odd mode drops to a minimum of 1.2323. At the same time, the difference between the x-polarized even and odd modes, which is 0.0007, is larger than the difference of 0.0004 between the y-polarized even and odd modes. This indicates that the coupling length of the

ISSN: 2414-1895 DOI: 10.6919/ICJE.202503_11(3).0004

x-polarized modes is shorter than that of the y-polarized modes, making it suitable for the fabrication of shorter couplers as sensor connectors.

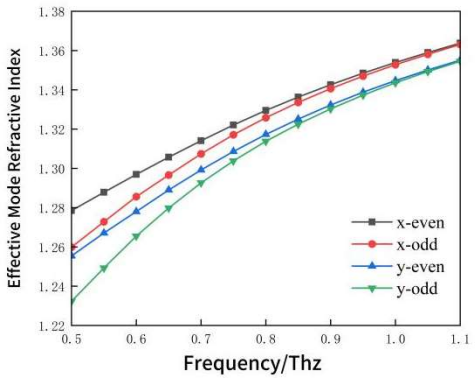

Fig. 3 Effective Mode Refractive Index Curve

The refractive index of the filling material is 1.376. By varying the major and minor axes of the core ellipse, the variation of the coupling length with frequency for different core ellipticity values ηis obtained.

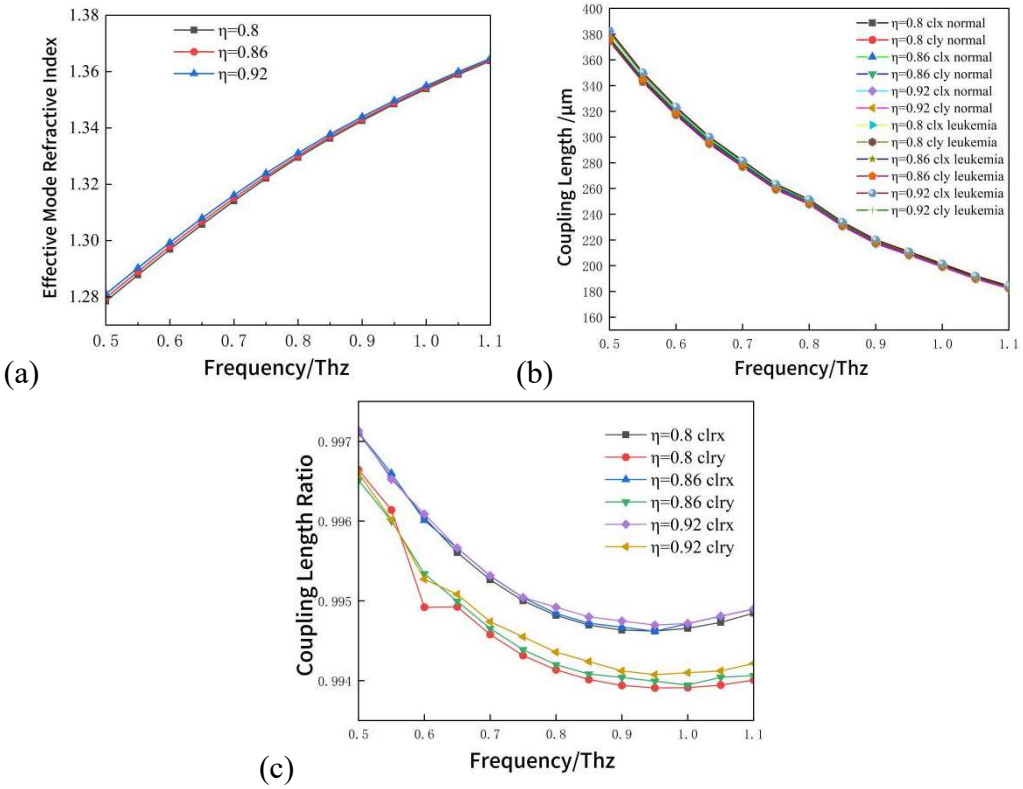

Fig. 4 Variation Curves for η = 0.8, 0.86, and 0.92.(a)Effective Refractive Index Variation Curve for Ellipticity of 0.8, 0.86, and 0.92.(b)Coupling Length vs Frequency Variation Curve.(c)Coupling Length Ratio vs Frequency Variation Curve.

Fig. 4(a) shows the variation of the effective refractive index of the x-polarized odd mode with frequency for core ellipticity values η = 0.8, 0.86, and 0.92 when the refractive index of the core filling material is n = 1.376. As seen from the figure, for a fixed core ellipticity η, the effective refractive index increases with the frequency and exhibits more noticeable changes over a larger frequency range. This is because the photonic crystal fiber (PCF) has a stronger confinement ability

ISSN: 2414-1895 DOI: 10.6919/ICJE.202503_11(3).0004

for higher-frequency modes. As the frequency increases, the confinement ability gradually strengthens, leading to a larger effective refractive index at higher frequencies. At the same frequency, the larger the ellipticity η, the larger the effective refractive index. This is because a higher η means the short axis of the elliptical air holes becomes smaller, reducing the relative air fraction, which concentrates the energy toward the core and confines it within the core. Therefore, η = 0.92 is chosen as the parameter for the photonic crystal fiber.

Fig. 4(b) shows the variation of the coupling length with frequency for different ellipticity values (η). From the figure, it can be observed that the coupling length decreases as the frequency increases. When the frequency increases from 0.5 THz to 1.1 THz, for both normal blood cells and leukemia cells, the coupling length decreases for ellipticity values of η = 0.8, 0.86, and 0.92. This behavior occurs because the increase in the ellipticity of the core enhances the structural asymmetry of the fiber. As the ellipticity η increases, the effective refractive index becomes larger, and the short axis of the elliptical air holes becomes smaller. This reduces the relative air fraction, thereby concentrating the energy more toward the core and confining it within the core. This results in a better coupling effect, leading to a shorter coupling length.

Fig. 4(c) shows the variation of the coupling length ratio with frequency. From the curve, it can be seen that the coupling length ratio is inversely proportional to the frequency, decreasing as the frequency increases. At the same frequency, as the ellipticity η increases, the structural asymmetry of the fiber increases, and the orthogonal asymmetry of the fiber cross-section becomes more pronounced. This leads to more energy being confined within the core. As a result, the coupling effect improves, and the coupling length becomes shorter.

The lattice constant, as a fundamental structural parameter, has an impact on the dual-core coupling effect in photonic crystal fibers. The study investigates the influence of different lattice constants (p) on the coupling length.

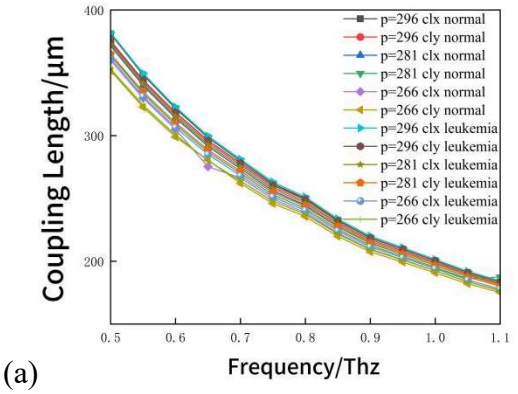

Fig. 5 Variation Curves for p = 296, 281, 266. (a) Coupling Length vs Frequency Variation Curve; (b) Coupling Length Ratio vs Frequency Variation Curve

ISSN: 2414-1895 DOI: 10.6919/ICJE.202503_11(3).0004

Fig. 5(a) shows the variation of the coupling length with frequency for η = 0.92, with core filling refractive indices of n = 1.376 and n = 1.39, and lattice constants p = 296, 281, and 261. From Figure 5(a), it can be observed that the coupling length decreases as the frequency increases, with a more noticeable trend at higher frequencies. This is because, at shorter wavelengths, the spatial distribution of electromagnetic waves becomes more compact, making it easier for interactions to occur between the photonic crystal fiber's air holes or periodic structures. This interaction enhances the coupling between different modes, leading to stronger mode coupling, shorter energy transfer distances, and consequently, shorter coupling lengths. At the same frequency, as the lattice constant p increases, the coupling length becomes larger. This is due to the fact that when the lattice constant increases, the spacing between the periodic structures also increases, weakening the interaction between light waves across different periodic units. As a result, the propagation distance required for coupling between modes becomes longer, leading to an increase in the coupling length.

Fig. 5(b) shows the variation of the coupling length ratio with frequency for η = 0.92, with core filling refractive indices of n = 1.376 and n = 1.39, and lattice constants p = 296, 281, and 261. From the curve, it can be observed that for p = 296, the coupling length ratio in the x-direction decreases as the frequency increases, reaching its minimum value of 0.99481 at 0.8 THz, after which it begins to rise slowly. This phenomenon occurs because, as the frequency increases, the wavelength of the light wave gradually shortens, and the coupler may experience increased mode losses or approach a point where further increases in frequency do not significantly affect the coupling ratio. At this point, the coupling length ratio stabilizes because the coupling capability of the fiber has reached its maximum. For p = 281 and p = 266, the coupling length ratio decreases with increasing frequency, gradually moving further from 1. Therefore, p = 266 is chosen as the optimal parameter for the photonic crystal fiber.

The diameter of the cladding air holes also has a significant impact on the coupling effect of photonic crystal fibers. Studies have shown that different cladding air hole diameters (d) can significantly affect the coupling length.

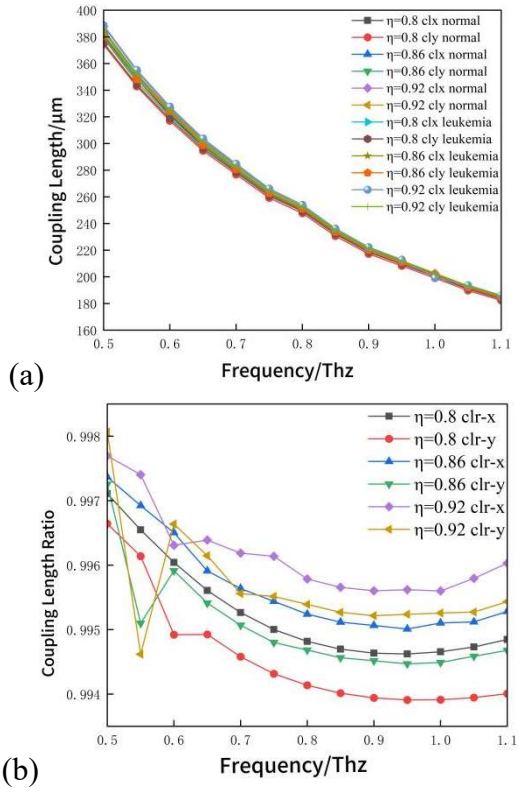

Fig. 6 Variation Curves for Cladding η = 0.8, 0.86, 0.92. (a) Coupling Length vs Frequency Variation Curve; (b) Coupling Length Ratio vs Frequency Variation Curve.

ISSN: 2414-1895 DOI: 10.6919/ICJE.202503_11(3).0004

As shown in Fig. 6(a), the coupling length of different cladding air holes decreases as the frequency increases. This is because the core tends to confine higher frequency modes, concentrating energy towards the core and restricting it within the core, resulting in better coupling effects and shorter coupling lengths. At the same frequency, when the short semi-axis of the cladding air holes increases, the coupling length becomes smaller. This is due to the enlargement of the air holes, which causes the light field to be more concentrated in the core, weakening the coupling strength.

According to Fig. 6(b), as the short semi-axis of the core ellipse increases, the mode field area of the fundamental mode decreases, while the width of the core coupling channel remains unchanged. This makes it easier for the optical energy to transfer from one core to another, thereby reducing the coupling length in both the x-polarized and y-polarized directions. As the air hole diameter increases, the effective refractive index of the four fundamental modes decreases, but the difference between the odd and even modes in the x and y polarizations increases, leading to a reduction in the coupling length. Although changes in the air hole diameter (d) significantly affect the coupling length in the x and y polarizations, its effect on the coupling length ratio is relatively small. Therefore, b2 = 150 μm is chosen as the parameter for the photonic crystal fiber.

Based on the given parameters core elliptic air hole $\eta = 0.92$, cladding elliptic air hole $\eta = 0.8$, lattice constant p = 266 μm, and coupling device length of 33,306 μm, the study shows that the refractive index of leukemia cells varies during different stages. In the early stage, the refractive index ranges from 1.38 to 1.42, in the mid-stage from 1.42 to 1.45, and in the late stage from 1.45 to 1.50 or higher. For this research, refractive indices of 1.39, 1.43, and 1.48 are selected for the early, mid, and late-stage cancer cells, respectively, along with a refractive index of 1.376 for normal blood cells. The normalized transmission power P_A and propagation distance relationship are then derived, as shown in Fig. 7.

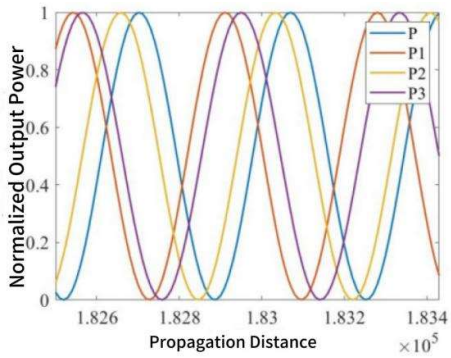

Fig. 7 Relationship between Normalized Transmission Power PA and Propagation Distance

The normalized output power of the fiber core, when incident light with a wavelength of 273 μm is emitted into the core, varies with propagation length, as shown in Figure 7. From the graph, it can be observed that at a propagation distance of 18,340 μm, the normalized output power of normal blood cells in the fiber core is 99.71%. At this point, the normalized power for early-stage cancer cells is 8.45%, for mid-stage cancer cells is 96.7%, and for late-stage cancer cells is 50.07%. Based on the normalized output power values, it is found that the power differences between early, mid, and late-stage cancer cells and normal blood cells are 91.26%, 3.01%, and 49.64%, respectively. This indicates that the sensor is highly sensitive in detecting early-stage cancer cells, while the measurement accuracy for mid-stage cancer cells needs further improvement. The sensor also demonstrates clear detection of late-stage cancer cells.This dual-core PCF (Photonic Crystal Fiber) structure sensor has significant potential for biochemical detection applications. By analyzing the shift in the central output wavelength, the coupling device's sensing performance can be optimized for early-stage cell analysis, providing more accurate and timely assistance in diagnosing and preventing the onset and progression of diseases.

ISSN: 2414-1895 DOI: 10.6919/ICJE.202503_11(3).0004

4. Conclusion

In this paper, a biosensor based on a dual-core photonic crystal fiber (PCF) structure is proposed, with Topas as the substrate material. Normal blood cells and cancerous blood cells are injected into the central air holes of the fiber. When terahertz waves propagate through the two fiber cores, the electric field interacts with the blood cells, affecting the coupling and sensing characteristics. By comparing different structural parameters, it is determined that when p=266, the elliptical hole between the cores has η=0.92, and the elliptical hole in the cladding has η=0.8, the shortest coupling length of 183.44 μm can be achieved. The normalized output power for early, middle, and late stages of cancer cells was measured, showing a 91.26% difference compared to normal blood cells, indicating that the sensor can effectively identify early-stage cancer cells. For late-stage cancer cells, the difference is 49.64% compared to normal blood cells, demonstrating that the sensor can also quickly detect late-stage cancer cells. This suggests that the studied dual-core photonic crystal fiber biosensor has significant potential for medical diagnostics.

References

[1] Yang, Y., Zhang, Z. Terahertz Imaging Technology. Beijing: Central University for Nationalities Press.2008.

[2] Liu, L., Jian, M., Chen, Y. Development of Terahertz Technology and Its Challenges in 6G Applications. ZTE Communications Technology,2021,27(02), 17-24.

[3] Yun-Peng W, Jin-Hui Y, et al. Design of a photonic crystal fiber polarization beam splitter with simple structure and ultra-wide bandwidth[J]. Chinese Physics B, 2023, 32(10).

[4] S. Suresh, Biomechanics and biophysics of cancer cells. Acta Biomater 3, 413–438 (2007). https:// doi. org/ 10. 1016/j. actbio. 2007.04. 002.

[5] M.J.B.M. Leon, M.A. Kabir, Design of a liquid sensing photonic crystal fiber with high sensitivity, birefringence & low confinement loss. Sens Bio-Sensing Res 28, 100335 (2020).

[6] Xiong, M., Huang, Y., Zhan, P., et al.. Bilateral D-shaped Photonic Crystal Fiber Surface Plasmon Temperature Sensor. Optical Communication Technology,2023, 47(2), 23-27.

[7] HOSSAIN M S, MOHAMMAD F. Theoretical Investigation of Mid Infrared Temperature Sensor Based on Sagnac Interferometer Using Chloroform Filled Photonic Crystal Fiber[J] IEEE sensors journal, 2021,21(21):24157-24165.

[8] M.J.B.M. Leon, M.A. Kabir, Design of a liquid sensing photonic crystal fiber with high sensitivity, birefringence & low confinement loss. Sens Bio-Sensing Res 28, 100335 (2020).

[9] HUSEYIN A, SHYQYRI H. PCF based sensor with high sensitivity, high birefringence and low confinement losses for liquid analyte sensing applications [J]. Sensors, 2015, 15(12):31833–31842.

[10] ARIF M F H, MD. BIDDUT M J H. Enhancement of relative sensitivity of photonic crystal fiber with high birefringence and low confinement loss [J]. Optik, 2017, 131: 697–704.

[11] LEON M J B M , KABRR M A. Design of a liquid sensing photonic crystal fiber with high sensitivity, birefringence & low confinement loss[J]. Sensing and Bio-Sensing Research, 2020, 28:100335.

[12] Zhao, L., Zhao, H., Xu, Z., et al.. A Design of Diagonal Symmetric Photonic Crystal Fiber for Chemical Sensing. Infrared and Millimeter Waves Journal, 2022, 41(1), 269-278.

[13] Du, H., Zheng, Y., & Pang, X. Design of Low-Loss Broadband Near-Zero Dispersion High Nonlinear Photonic Crystal Fiber. High Power Laser and Particle Beams,2021, 33(09), 28-34.

[14] Islam M S, Sultana J, Dinovitser A, et al. A novel Zeonex based oligoporous-core photonic crystal fiber for polarization preserving terahertz applications[J]. Optics Communications, 2018, 413: 242-248.

[15] Islam M R, Kabir M F, Talha K M A, et al. Highly birefringent honeycomb cladding terahertz fiber for polarization-maintaining applications[J]. Optical Engineering, 2020, 59(1): 016113-016113.

[16] Ademgil H, Haxha S. PCF based sensor with high sensitivity, high birefringence and low confinement losses for liquid analyte sensing applications[J]. Sensors, 2015, 15(12): 31833-31842.